Iron spin state in silicate perovskite at conditions of the Earth's deep interior

Catherine McCammon[a], Konstantin Glazyrin[a], Anastasia Kantor[ab],
Innokenty Kantor[b], Ilya Kupenko[ab], Olga Narygina[a], Vasily
Potapkin[abc], Clemens Prescher[a], Ryosuke Sinmyo[a], Alexandr
Chumakov[bc], Rudolf Rüffer[b], Ilya Sergueev[b], Gennady Smirnov[c] &
Leonid Dubrovinsky[a]

[a] Bayerisches Geoinstitut, Universität Bayreuth, Bayreuth,
Germany

[b] European Synchrotron Radiation Facility, Grenoble, France

[c] National Research Center "Kurchatov Institute", Moscow, Russia
Published online: 11 Jun 2013.

PLEASE SCROLL DOWN FOR ARTICLE

Taylor & Francis
Taylor & Francis Group

REVIEW

Iron spin state in silicate perovskite at conditions of the Earth's deep interior[†]

Catherine McCammon[a]*, Konstantin Glazyrin[a], Anastasia Kantor[a,b], Innokenty Kantor[b],
Ilya Kupenko[a,b], Olga Narygina[a], Vasily Potapkin[a,b,c], Clemens Prescher[a], Ryosuke Sinmyo[a],
Alexandr Chumakov[b,c], Rudolf Rüffer[b], Ilya Sergueev[b], Gennady Smirnov[c]
and Leonid Dubrovinsky[a]

[a]*Bayerisches Geoinstitut, Universität Bayreuth, Bayreuth, Germany;* [b]*European Synchrotron Radiation Facility, Grenoble, France;* [c]*National Research Center "Kurchatov Institute", Moscow, Russia*

We present a review of our recent work concerning the spin state of Fe^{2+} and Fe^{3+} in iron magnesium aluminium silicate perovskite, the most abundant phase in the Earth's interior. Experimental results obtained using Mössbauer spectroscopy (with a radioactive source and a Synchrotron Mössbauer Source) and nuclear forward scattering for a range of different sample compositions in both externally heated and laser-heated diamond anvil cells show clear trends in the variation of hyperfine parameters with pressure and temperature. These trends combined with reported total spin state measurements using X-ray emission spectroscopy on samples of similar composition support the conclusion that Fe^{2+} undergoes a high-spin to intermediate-spin transition near the top of the lower mantle and an intermediate-spin to low-spin transition near the bottom of the lower mantle. No spin transition is observed to occur in Fe^{3+} for samples with compositions relevant for the lower mantle.

Keywords: Mössbauer spectroscopy; spin transition; lower mantle; diamond anvil cell

1. Introduction

The lower mantle, which constitutes more than half of the Earth's volume, consists predominantly of $(Mg,Fe)(Si,Al)O_3$ perovskite (hereafter referred to as FePv), making this phase the most abundant in the Earth's interior. The physical and chemical properties of FePv largely determine those of the lower mantle, which strongly influences the dynamics and evolution of the Earth's interior through geological time. Although iron is a minor constituent, its ability to adopt different valence and spin states can significantly influence the properties of FePv. Current models suggest that at least half of the iron in FePv is Fe^{3+},[1–3] indicating that spin transitions in either Fe^{2+} or Fe^{3+} (or both) are relevant for lower mantle behaviour.

The perovskite structure is well known in many research fields and can incorporate more than half of the elements in the periodic table. The structure contains two sites, a large dodecahedral site (which is distorted to 8–12 coordination in FePv) (designated "A") and a smaller octahedral
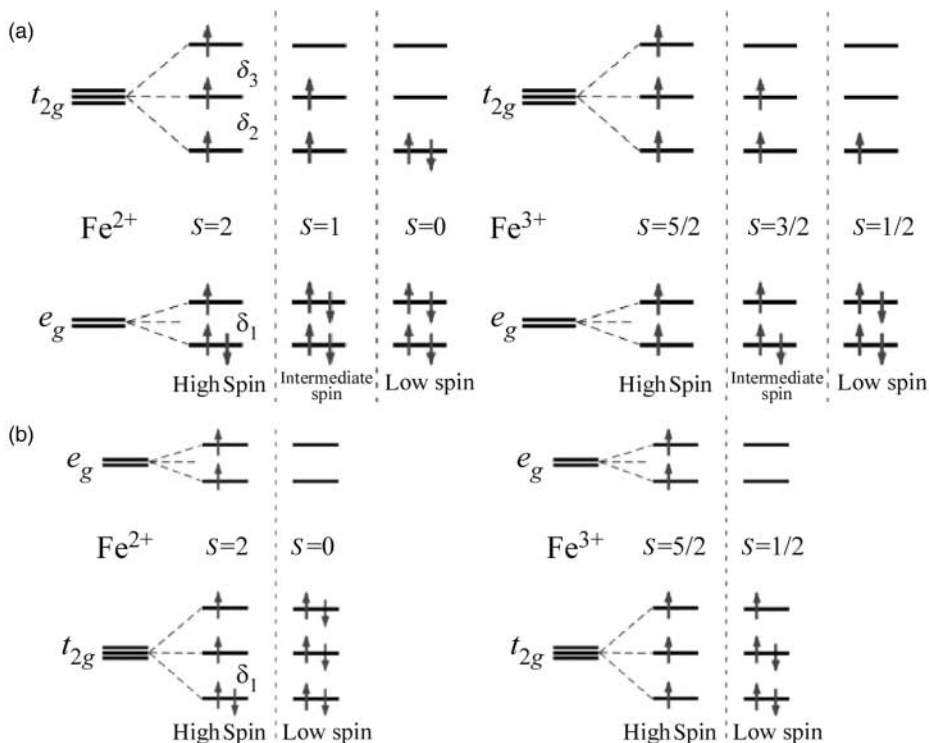
Figure 1. Schematic diagram showing possible electron configurations for Fe^{2+} and Fe^{3+} in the perovskite structure occupying (a) the A-site and (b) the B-site.

site ("B"). The A-site is primarily occupied by Mg^{2+}, while the B-site is dominated by Si^{4+} and is the preferred site for Al^{3+}. Fe^{2+} occupies exclusively the A-site, and while Fe^{3+} can occupy both the A-site and the B-site, for lower mantle compositions where Al^{3+} is also present and occupies the B-site, Fe^{3+} is observed to occupy exclusively the A-site.[4]

The distribution of d electrons of Fe^{2+} and Fe^{3+} in the A- and B-sites of FePv determines their individual spin states [5] (Figure 1). In the high-spin (HS) state the electrons are distributed among the maximum number of orbitals possible, while in the low-spin (LS) state the electrons occupy orbitals with the lowest possible energy. An intermediate-spin (IS) state where electrons are only partially spin-paired can be stable in particular coordination environments.[6]

A number of experimental methods have been used to study the nature of spin transitions in FePv. X-ray emission spectroscopy (XES) provides a measure of the number of unpaired d electrons through the intensity of a satellite peak on the low energy shoulder of the main emission line [7] and has been used by many groups to investigate spin transitions involving iron in various compositions of FePv.[8–15] All of these studies observed a decrease in the unpaired spin density of iron in FePv, although there is no general consensus as to whether Fe^{2+} or Fe^{3+} or both are involved in the spin transition(s). To resolve individual contributions to the unpaired spin density, Mössbauer spectroscopy can be used to track changes in hyperfine parameters as a function of pressure and/or temperature. The method can be applied in the laboratory using a radioactive source, or at a third-generation synchrotron.[16] The former enables measurements to be performed in the energy domain, while the latter provides the opportunity for measurements in both the time domain (nuclear forward scattering (NFS)) (*e.g.* [17] and references therein) and the energy domain (Synchrotron Mössbauer Source (SMS)).[18] In this paper, we summarise results of our recent Mössbauer work on FePv and present a new appraisal of hyperfine parameters and

Table 1. Chemical composition and experimental details of samples investigated using Mössbauer spectroscopy.

Composition	$Fe^{3+}/\Sigma Fe$	Species present	P range	T range	Ref.
$Mg_{0.88(1)}Fe_{0.12(1)}Si_{1.00(1)}O_3$ pv	15(3)%	$^{A}Fe^{2+}$; $^{A}Fe^{3+}$; $^{B}Fe^{3+}$?	0–89 GPa	300–800 K	[19]
$Mg_{0.86(1)}Fe_{0.14(1)}Si_{0.98(1)}Al_{0.020(5)}O_3$ pv	30(5)%	$^{A}Fe^{2+}$; $^{A}Fe^{3+}$; $^{B}Fe^{3+}$?	0–55 GPa	300–700 K	[19]
$Mg_{0.82(1)}Fe_{0.18(1)}Si_{1.00(1)}O_3$ pv	17(5)%	$^{A}Fe^{2+}$; $^{A}Fe^{3+}$; $^{B}Fe^{3+}$?	0–130 GPa	300–1000 K	[20]
$Mg_{0.60(3)}Fe_{0.40(3)}Si_{0.63(3)}Al_{0.37(2)}O_3$ pv	80(5)%	$^{A}Fe^{2+}$; $^{A}Fe^{3+}$	3–93 GPa	300 K	[22]
$Mg_{0.60(3)}Fe_{0.40(3)}Si_{0.63(3)}Al_{0.37(2)}O_3$ pv	70(5)%	$^{A}Fe^{2+}$; $^{A}Fe^{3+}$	4–78 GPa	300 K	[22]
$Mg_{0.828(18)}Fe_{0.208(13)}Si_{0.911(23)}Al_{0.059(2)}O_3$ pv	50(5)%	$^{A}Fe^{2+}$; $^{A}Fe^{3+}$	26–122 GPa	300 K	[22]
$Mg_{0.946(17)}Fe_{0.056(12)}Si_{0.997(16)}O_3$ pv	20(5)%	$^{A}Fe^{2+}$; $^{A}Fe^{3+}$	4–75 GPa	300 K	[22]
$Mg_{0.82(1)}Fe_{0.18(1)}Si_{1.00(1)}O_3$ majorite	10(3)%	$^{[8]}Fe^{2+}$; $^{[6]}Fe^{2+}$; $^{[6]}Fe^{3+}$	2–52 GPa	300–670 K	[21]

pv, perovskite.

their relation to iron spin state to produce a more comprehensive picture of iron spin state in the lower mantle.

2.   Experimental methods

Our studies involved measurements of FePv with different compositions at a range of pressure and temperature conditions, which are summarised in Table 1. Samples were loaded into diamond anvil cells (DAC), where some incorporated a resistive heater, and some were mounted on a stage enabling laser heating; further details are given in the original references.[19–22]

^{57}Fe Mössbauer spectra were collected at Bayerisches Geoinstitut using a constant acceleration Mössbauer spectrometer equipped with a high-specific activity point source (500 μm active diameter) with 370 MBq nominal activity. The velocity scale was calibrated relative to α-Fe. ^{57}Fe NFS data were collected on the Nuclear Resonance beamline (ID18) [23] at the European Synchrotron Radiation Facility (ESRF) during operation in 4-bunch and 16-bunch modes with the beam focused to ~$10 \times 10\,\mu m^2$ using a Kirkpatrick-Baez mirror. ^{57}Fe Mössbauer spectra were collected using SMS methodology on beamline ID18 at the ESRF during operation in 7/8 + 1 multibunch mode with the beam focused to ~$10 \times 10\,\mu m^2$ using a Kirkpatrick-Baez mirror. The linewidth of the source was controlled before and after each measurement using $K_2Mg^{57}Fe(CN)_6$ (single-line absorber) and the velocity scale was calibrated relative to α-Fe. Further details of the SMS methodology are given in the literature.[18]

Mössbauer spectra were fitted using the program MossA.[24] A Lorentzian source lineshape was used for Mössbauer spectra collected using a radioactive source, while a normalised squared Lorentzian source lineshape was used for SMS spectra.[25] The full transmission integral was used for conventional Mössbauer spectra of thick samples and for all SMS spectra. Conventional constraints for quadrupole doublets were used (component doublet widths and areas constrained to be equal), except in the case of preferred orientation, where the effect was more prominent in SMS spectra due to the polarised nature of the source. For these cases, the component areas were allowed to vary, with all area ratios of doublets within a single spectrum constrained to be the same based on the reasonable assumption that the principal directions of the electric field gradient (EFG) for Fe^{2+} and Fe^{3+} for both sites of the perovskite structure are the same based on its crystallography. NFS spectra were fitted using the program MOTIF.[26]

3.   Results

The starting point for the interpretation of spin states in Mössbauer and NFS spectra of FePv are the hyperfine parameters (centre shift (CS) and quadrupole splitting (QS)) corresponding to the
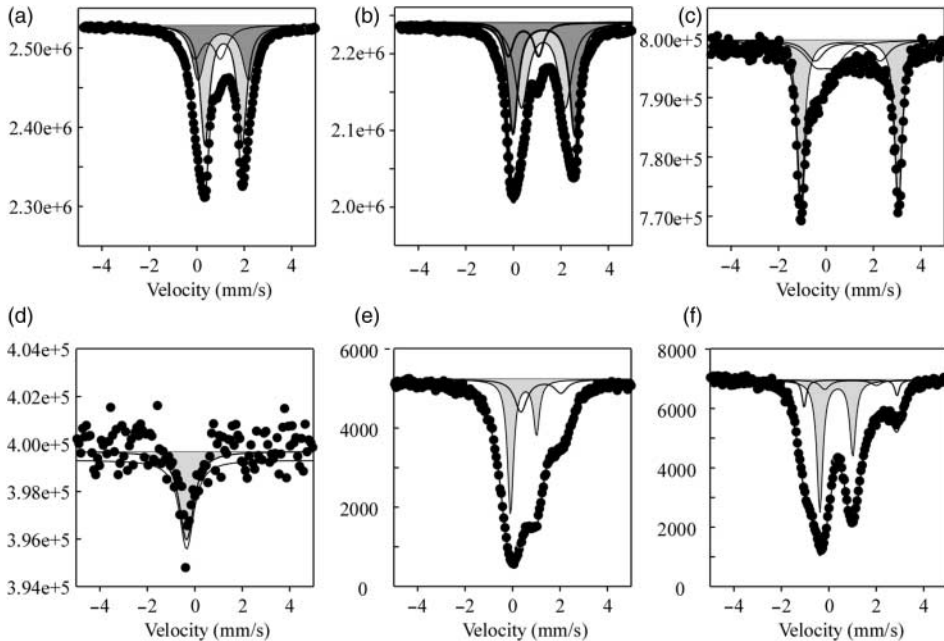
Figure 2. Room temperature Mössbauer spectra of FePv: (a) $Mg_{0.91}Fe_{0.09}SiO_3$ at 0 GPa showing two different quadrupole doublets arising from HS Fe^{2+} (grey, dark grey) (data from [30]); (b) $Mg_{0.91}Fe_{0.09}SiO_3$ at 0 GPa and 80 K where low temperature changes the relative areas of the two quadrupole doublets arising from HS Fe^{2+} (grey, dark grey) (data from [30]); (c) $Mg_{0.91}Fe_{0.09}SiO_3$ at 74 GPa dominated by high QS Fe^{2+} (grey) (data from [19]); (d) $Mg_{0.82}Fe_{0.18}SiO_3$ at 130 GPa dominated by low CS Fe^{2+} (grey) (data from [20]); (e) $Mg_{0.6}Fe_{0.4}Si_{0.63}Al_{0.37}O_3$ at 2 GPa dominated by HS Fe^{3+} (grey) (data from [22]); (f) $Mg_{0.6}Fe_{0.4}Si_{0.63}Al_{0.37}O_3$ at 93 GPa dominated by HS Fe^{3+} (grey) (data from [22]). Spectra (a)–(d) were collected using a radioactive source, while (e) and (f) were collected using SMS methodology. Area asymmetry in (e) and (f) is due to preferred orientation of the sample coupled with the polarised nature of the SMS. All spectra were collected at 300 K unless otherwise noted.

different components and their trends with pressure and temperature. All components observed at ambient conditions are taken to correspond to HS configurations.

Mössbauer spectra of FePv dominated by HS Fe^{2+} show two main absorption peaks at ambient conditions (Figure 2(a)). Although the simplest fit of the HS Fe^{2+} absorption is a single quadrupole doublet, many studies report the presence of broadening, asymmetry and/or distinct shoulders on the main peaks that indicate the presence of more than one discrete set of hyperfine parameters. The best fits have been obtained using two doublets with similar CS but slightly different QS values (one < 2 mm/s and one > 2 mm/s), and all studies made at ambient temperature and variable temperature report that the relative intensity of the doublet with larger splitting increases with decreasing temperature (Figure 2(b)).[27–30] Increasing pressure also appears to have a similar effect as decreasing temperature on the relative intensities [19,21]; however, the individual intensities of the HS Fe^{2+} doublets become difficult to resolve above ~ 30 GPa due to the appearance of a new component.

The quadrupole doublet (hereafter referred to as "high QS Fe^{2+}") that appears above ~ 30 GPa in FePv Mössbauer and NFS spectra has a narrow linewidth and CS similar to that for HS Fe^{2+}, but significantly higher QS (> 4 mm/s). The intensity of the high QS Fe^{2+} doublet increases rapidly with pressure until it dominates Fe^{2+} absorption above ~ 50 GPa (Figure 2(c)), and it is stabilised with increasing temperature as shown by Mössbauer and NFS spectra collected during DAC experiments involving external and laser heating.[19,21,31] Notably the high QS Fe^{2+} doublet has been observed in all high pressure nuclear resonance studies of FePv containing Fe^{2+},[10,19–22,31–34] even though its interpretation is still the subject of discussion (see below).

At even higher pressures (> 115 GPa), another new component appears in Mössbauer and NFS spectra of FePv that is associated with Fe^{2+}, because its intensity grows with increasing pressure at the expense of the high QS Fe^{2+} doublet (Figure 2(d)).[20] Increasing temperature also increases the stability of this new component (referred to as "low CS Fe^{2+}"), where all Fe^{2+} in FePv was observed to transform to low CS Fe^{2+} at 120 GPa and 1000 K.[20]

Mössbauer spectra of FePv dominated by HS Fe^{3+} show two main absorption peaks at ambient conditions (Figure 2(e)). In the case where Fe^{3+} occupies exclusively the A-site ($^A Fe^{3+}$), HS Fe^{3+} absorption in all spectra can be fit at ambient conditions to a single quadrupole doublet with CS ~ 0.4 mm/s and QS ~ 1 mm/s.[22] Similar hyperfine parameters for HS Fe^{3+} in the B-site ($^B Fe^{3+}$) have been reported from NFS spectra.[34] However, the Mössbauer spectra of FePv samples with low Fe^{3+}/Σ Fe and $^B Fe^{3+}$ can be complicated by the presence of Fe^{2+}–Fe^{3+} electron delocalisation across the $^A Fe^{2+}$–$^B Fe^{3+}$ shared face,[35] which can result in a doublet with CS and QS values intermediate between Fe^{2+} and Fe^{3+}.[29,36]

The hyperfine parameters of the $^A Fe^{3+}$ doublet change negligibly with increasing pressure, despite the appearance of the high QS Fe^{2+} doublet above 30 GPa.[22] Even at the highest pressures reached, $^A Fe^{3+}$ absorption does not change significantly from its appearance at ambient conditions (Figure 2(f)). For $^B Fe^{3+}$ absorption, several groups have reported an increase in QS to values of up to 3 mm/s occurring at pressures variously between 20 and 70 GPa (depending on the study).[13,14,34]

4. Discussion

4.1. *Spin state assignments*

The relative areas of Mössbauer components can be used to calculate the total spin state (*i.e.* average number of unpaired d electrons) based on the different possibilities for assigning doublet components to spin state. Here, $S_T = \Sigma S_n \times A_n$, where S_n is the spin number assigned to the *n*th doublet with relative area A_n, and the sum is over all *n* doublets. The calculated value of S_T can then be compared with the value of S_T determined independently for similar FePv compositions using XES.[8,9] These calculations were performed based on the hyperfine parameters taken from 94 Mössbauer and NFS spectra collected between 0 and 110 GPa at room temperature for six possible models: assignment of the high QS Fe^{2+} doublet to HS, IS or LS and assignment of the weak Fe^{3+} doublet to either HS or LS.[19] Of these models, one fits the XES data almost exactly (high QS Fe^{2+} assigned to IS and Fe^{3+} assigned to HS), a second gave S_T values that were only slightly different to XES data (high QS Fe^{2+} assigned to IS and Fe^{3+} assigned to LS), while the other four models (involving the high QS Fe^{2+} doublet assigned to either HS Fe^{2+} or LS Fe^{2+}) gave S_T values that were totally inconsistent with XES data. Further support for the assignment of the high QS Fe^{2+} doublet to IS Fe^{2+} is provided by the observed stabilisation of the high QS Fe^{2+} doublet at high temperature and high pressure,[19,21,31] which is consistent with XES measurements on an FePv sample with similar composition at 108 GPa and temperatures up to ~ 3000 K that shows a total spin state near one.[31] Hence, the most plausible assignment of the high QS Fe^{2+} doublet based on experimental studies is IS Fe^{2+}.[12,19,31]

The appearance of the low CS Fe^{2+} component above 115 GPa (Figure 2(d)) coincides with a large decrease in spin density shown by XES measurements on Fe^{2+}-rich FePv.[8,12] This component is therefore assigned to LS Fe^{2+}.[12,20]

The hyperfine parameters of the $^A Fe^{3+}$ doublet do not change significantly with pressure up to at least 122 GPa; hence, $^A Fe^{3+}$ is inferred to remain in the HS state throughout this pressure range.[22] Other studies on FePv with $^B Fe^{3+}$ present report changes in the NFS spectra, a decrease in cell volume, and a decrease in the total spin state observed using XES at pressures variously

in the range 20 and 70 GPa (depending on the study).[13–15,34] These results support an HS–LS transition in $^B Fe^{3+}$. However, Fe^{3+} is expected to occupy only the A-site in lower mantle FePv due to the presence of Al^{3+} (which preferentially occupies the B-site),[4] which would rule out the presence of an HS–LS transition of Fe^{3+} in the lower mantle. Some studies have suggested that the reduced volume of LS $^B Fe^{3+}$ could lead to a redistribution of Fe^{3+} from the A- to the B-site, hence causing an HS–LS transition [13–15]; however, this possibility has been ruled out by repeated laser annealing of several FePv samples at high pressure that showed that Fe^{3+} remains on the A-site in FePv even at lower mantle conditions.[22]

4.2. *Comparison with theoretical calculations*

Parallel to the experimental studies of FePv spin state at high pressure, theoretical calculations have been carried out to determine the stable spin configurations of Fe^{2+} and Fe^{3+} in the perovskite structure.[37–48] As summarised in a recent review,[49] theoretical calculations of Fe^{3+} in FePv are broadly consistent with experimental results, predicting a stable HS configuration for $^A Fe^{3+}$ at pressures throughout the lower mantle, and an HS–LS transition in $^B Fe^{3+}$ at pressures roughly similar to those reported in experimental studies. Many theoretical studies have predicted an HS–LS transition of Fe^{2+} at very high pressures,[37,40–43,45,47] even though transition pressures vary depending on a number of factors including the choice of exchange-correlation energy.[46,49]

In contrast to the HS and LS states, the existence of IS Fe^{2+} has been extremely controversial. No theoretical calculations of Fe^{2+} in FePv have ever found any Fe^{2+} IS configurations to be stable,[50] and alternative explanations have been given in some experimental reports for the decrease in satellite peak intensity observed in XES data,[8,9] such as an HS–LS transition of minority Fe^{3+} [10,32,34] or an HS–LS transition of Fe^{2+}.[8,33] Several theoretical studies have reported the presence of two different stable local atomic configurations of HS Fe^{2+} in the A-site where QS values > 3 mm/s have been calculated for the configuration that is stable at higher pressure.[44,45] However, such an assignment of high QS Fe^{2+} to HS Fe^{2+} is difficult to reconcile with the decrease in satellite peak intensity observed in XES data [8,9] and, based on our results, would require either the presence of impurities in samples examined using XES or a reinterpretation of the XES data.

4.3. *QS and spin state*

The hyperfine parameter ranges of Fe^{2+} and Fe^{3+} from high pressure measurements of FePv provide further insight into their site and spin state assignments (Figure 3). A useful comparison comes from analogous high pressure measurements carried out on a sample of majorite [21] (Table 1), since the majorite structure (which is based on the garnet structure) contains $^{[8]}Fe^{2+}$ (*i.e.* dodecahedral coordination), $^{[6]}Fe^{2+}$ and $^{[6]}Fe^{3+}$ (*i.e.* octahedral coordination). The remarkably high QS values for the IS Fe^{2+} doublet in FePv are similar to those for HS $^{[8]}Fe^{2+}$ in majorite (Figure 3), which has led to suggestions in the literature that the high QS Fe^{2+} doublet in FePv must correspond to the HS state. However, as demonstrated by Narygina et al.,[21] the origins of the QS values for FePv and majorite are quite different.

Briefly, the QS is determined by two factors: (a) a lattice contribution which is proportional to the EFG produced by electrons in atoms adjacent to the absorbing nucleus and (b) a valence contribution which is proportional to the EFG produced by the valence electrons of the absorbing nucleus.[51] For Fe^{2+} electron configurations with one or more unpaired d electrons, the valence contribution to the EFG is usually an order of magnitude larger than the lattice contribution; hence, the valence contribution dominates QS.[51] For $^{[8]}Fe^{2+}$ in majorite (which has the same electronic structure as the $Fe^{2+} S = 2$ case in Figure 1(a)), the main contribution to the EFG
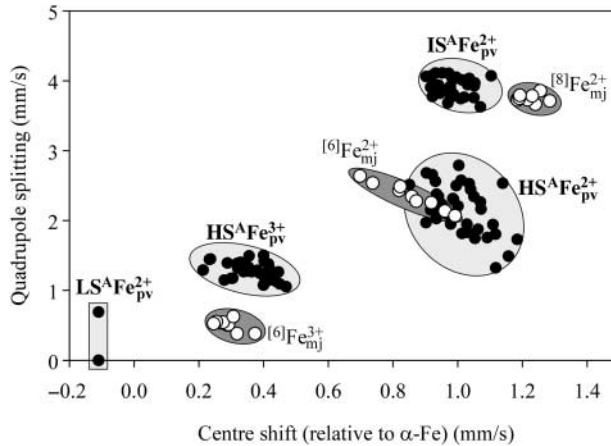
Figure 3. Hyperfine parameter ranges of FePv and (Mg,Fe)SiO$_3$ majorite from Mössbauer spectra collected at 300 K and pressures up to 120 GPa. Data are taken from [22] (solid circles) and [21] (open circles); details of composition and pressure ranges for each dataset are given in Table 1. Ranges for FePv and majorite are shaded light grey and dark grey, respectively.

arises from the unequal population of the lowest energy orbitals (e_g), which is proportional to their energy difference, δ_1 (Figure 1(a)). The value of δ_1 can be determined from the temperature dependence of QS [52] and was calculated to be $\sim 1500\,\mathrm{cm}^{-1}$ for Mg$_{0.82}$Fe$_{0.18}$SiO$_3$ majorite.[21] This value for Fe^{2+} is extremely high compared with the ground state splitting for other silicate minerals [5] and explains the extremely high value of QS observed for $^{[8]}$Fe^{2+} in majorite. In contrast, the value of δ_1 for HS ^{A}Fe^{2+} in FePv (which has the same electronic structure as $^{[8]}$Fe^{2+} in majorite) has been estimated from optical absorption spectra to be only $\sim 500\,\mathrm{cm}^{-1}$.[35] This lower value of δ_1 results in a lower value of QS, as seen in Figure 3 for HS ^{A}Fe^{2+}. Indeed the range of experimentally observed QS values for HS ^{A}Fe^{2+} nearly covers the values found in theoretical calculations of HS ^{A}Fe^{2+} [44,45,49]; hence, the two different local atomic configurations of HS ^{A}Fe^{2+} predicted by theory may correspond to the two doublets shown in Figure 2(a) and 2(b), where the doublet with higher QS becomes more stable at both reduced temperature and elevated pressure, the latter according to theory predictions.

In the case of IS ^{A}Fe^{2+}, the lower lying e_g levels are completely filled; hence, it is the asymmetry caused by the splitting of the upper t_{2g} levels (δ_2) that determines the QS (Figure 1(a), $S = 1$). Optical absorption spectra show that the upper level splitting (δ_2) in FePv is significantly higher than the ground-level splitting (δ_1),[35] consistent with observations for Fe^{2+} in many other minerals.[5] QS for IS ^{A}Fe^{2+} should therefore be larger than that for HS ^{A}Fe^{2+},[21] which is consistent with experimental observations (Figure 3).

The relative magnitude of QS values for $^{[8]}$Fe^{2+} and $^{[6]}$Fe^{2+} in majorite can also be explained by the above considerations. The electronic structure of the former is the $S = 2$ configuration in Figure 1(a), while for the latter it is the $S = 2$ configuration in Figure 1(b). The relatively low distortion of the six-fold site in majorite leads to a low value of δ_1,[5] compared to the significantly higher value of $1500\,\mathrm{cm}^{-1}$ determined for the eight-fold site. This difference in δ_1 values is reflected in the lower QS values observed for $^{[6]}$Fe^{2+} in majorite (Figure 3).

In the case of HS Fe^{3+}, the valence contribution to the EFG is zero due to the symmetric distribution of the five d electrons among the five d orbitals (Figure 1); hence, QS is determined solely by the lattice contribution.[51] To a first approximation, the lattice contribution provides a measure of the degree of distortion of the atomic environment; hence, the higher QS values of HS ^{A}Fe^{3+} in FePv compared to $^{[6]}$Fe^{3+} in majorite can be taken to indicate a larger distortion of the A-site in the perovskite structure compared to the six-fold site in majorite.
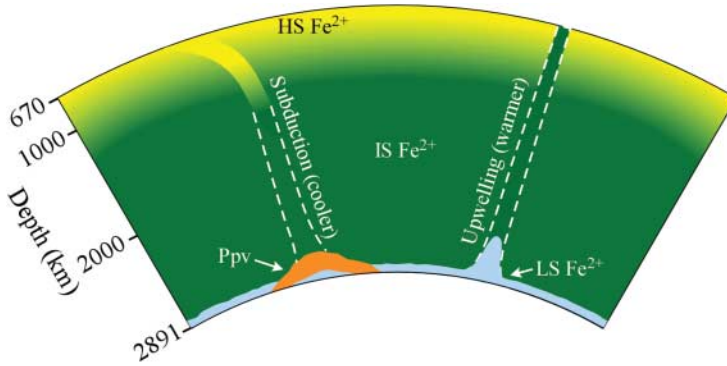
Figure 4. Distribution of iron spin states in FePv in the lower mantle based on our experimental results.[19–22] The HS, IS and LS states of Fe^{2+} are indicated by yellow, green and blue, respectively, while the post-perovskite phase is indicated by orange. Fe^{3+} in FePv is predicted to remain in the HS state throughout the entire lower mantle (colour online only).

In the case of LS Fe^{2+}, the $S = 0$ electron configuration (Figure 1) implies a negligible valence contribution to the EFG, and hence a low value of QS (Figure 3). In contrast, the highly asymmetric electron distribution of the LS state of Fe^{3+} ($S = 1/2$ configurations in Figure 1) is predicted to give a high value of QS. This is consistent with experimental observations of QS values in the range 2–3.5 mm/s [13,14,34] and theoretical calculations of QS values in the range 2–3 mm/s.[48]

4.4. *Spin state model for the lower mantle*

The results from our experimental studies can be used to construct a more comprehensive model for iron spin state in lower mantle FePv (Figure 4). The Fe^{2+} HS–IS transition in FePv starts at relatively low pressure (~ 30 GPa) and the Fe^{2+} IS state is stabilised by increasing temperature [19,21]; therefore, HS Fe^{2+} is expected to occur only at the top of the lower mantle. The effect of temperature on the HS–IS transition of Fe^{2+} in FePv is observed to be greater than the effect of composition [19]; hence, downgoing slabs in the uppermost lower mantle are predicted to contain more HS Fe^{2+} compared with the surrounding mantle owing to their lower temperatures, whereas areas of mantle upwelling are inferred to contain more IS Fe^{2+} owing to their higher temperatures (Figure 4). The Fe^{2+} IS–LS transition in FePv starts at high pressure (> 100 GPa) and the Fe^{2+} LS state is stabilised by increasing temperature [20]; therefore, LS Fe^{2+} is expected to occur only at the bottom of the lower mantle. In hot regions such as upwelling plumes, the IS–LS transition is predicted to take place at shallower depths, while in cold regions such as those expected in the case of large accumulations of subducted material, FePv is predicted to transform to the post-perovskite (Ppv) phase (reviewed by [53]). If a double crossing of the FePv–Ppv transition occurs as proposed just above the core–mantle boundary,[54] the Ppv phase is predicted to transform to FePv containing LS Fe^{2+}.[20]

5. Conclusions and outlook

Our work has shown that for lower mantle FePv, there are profound changes in Mössbauer and NFS spectra of FePv that can be explained by changes in the spin state of Fe^{2+}, while no spin transitions occur in Fe^{3+}. These results are consistent with electrical conductivity studies that show a conductivity drop in Fe^{2+}-rich compositions, but no drop in those rich in Fe^{3+} ([22] and references therein), and combined with recent results reporting the influence of Fe^{3+} in elastic

wave velocities of FePv,[55] they may provide improved constraints for forward modelling of electromagnetic data as well as for joint inversion of electromagnetic and seismic data.

Acknowledgements

References

[1] McCammon CA. Perovskite as a possible sink for ferric iron in the lower mantle. Nature. 1997;387:694–696.
[2] Frost DJ, Liebske C, Langenhorst F, McCammon CA, Trønnes R, Rubie DC. Experimental evidence for the existence of iron-rich metal in the Earth's lower mantle. Nature. 2004;428:409–411.
[3] McCammon CA. The paradox of mantle redox. Science. 2005;308:807–808.
[4] Vanpeteghem CB, Angel RJ, Ross NL, Jacobsen SD, Dobson DP, Litasov KD, Ohtani E. Al, Fe substitution in the $MgSiO_3$ perovskite structure: a single-crystal X-ray diffraction study. Phys Earth Planet Inter. 2006;155:96–103.
[5] Burns RG. Mineralogical applications of crystal field theory. 2nd ed. Cambridge, UK: Cambridge University Press; 1993.
[6] Alvarez S, Cirera J. How high the spin? Allowed and forbidden spin states in transition-metal chemistry. Angewandte Chemie International Edition. 2006;45:3012–3020.
[7] Vankó G, Neisius T, Molnár G, Renz F, Kárpáti S, Shukla A, Groot FMFd. Probing the 3d spin momentum with X-ray emission spectroscopy: the case of molecular-spin transitions. J Phys Chem B. 2006;110:11647–11653.
[8] Badro J, Rueff JP, Vanko G, Monaco G, Fiquet G, Guyot F. Electronic transitions in perovskite: possible non-convecting layers in the lower mantle. Science. 2004;305:383–386.
[9] Li J, Struzhkin VV, Mao H-K, Shu J, Hemley RJ, Fei Y, Mysen B, Dera P, Prakapenka V, Shen G. Electronic spin state of iron in lower mantle perovskite. Proc Natl Acad Sci. 2004;101:14027–14030.
[10] Li J, Sturhahn W, Jackson JM, Struzhkin VV, Lin JF, Zhao J, Mao HK, Shen G. Pressure effect on the electronic structure of iron in (Mg,Fe)(Si,Al)O_3 perovskite: a combined synchrotron Mössbauer and X-ray emission spectroscopy study up to 100 GPa. Phys Chem Miner. 2006;33:575–585.
[11] Lin J-F, Watson H, Vankó G, Alp EE, Prakapenka VB, Dera P, Struzhkin VV, Kubo A, Zhao J, Mccammon C, Evans WJ. Intermediate-spin ferrous iron in lowermost mantle post-perovskite and perovskite. Nat Geosci. 2008;1:688–691.
[12] Lin J-F, Speziale S, Prakapenka VB, Dera P, Lavina B, Watson HC. High-pressure X-ray diffraction and X-ray emission studies on iron-bearing silicate perovskite under high pressures. High Press Res. 2010;30:230–237.
[13] Catalli K, Shim S-H, Prakapenka VB, Zhao J, Sturhahn W, Chow P, Xiao Y, Liu H, Cynn H, Evans WJ. Spin state of ferric iron in $MgSiO_3$ perovskite and its effect on elastic properties. Earth Planet Sci Lett. 2010;289:68–75.
[14] Catalli K, Shim S-H, Dera P, Prakapenka VB, Zhao J, Sturhahn W, Chow P, Xiao Y, Cynn H, Evans WJ. Effects of the Fe^{3+} spin transition on the properties of aluminous perovskite – new insights for lower-mantle seismic heterogeneities. Earth Planet Sci Lett. 2011;310:293–302.
[15] Fujino K, Nishio-Hamane D, Seto Y, Sata N, Nagai T, Shinmei T, Irifune T, Ishii H, Hiraoka N, Cai YQ, Tsuei K-D. Spin transition of ferric iron in Al-bearing Mg–perovskite up to 200 GPa and its implication for the lower mantle. Earth Planet Sci Lett. 2012;317–318:407–412.
[16] Gütlich P, Bill E, Trautwein A. Mössbauer spectroscopy and transition metal chemistry. Berlin: Springer-Verlag; 2011.
[17] Sturhahn W. Nuclear resonant spectroscopy. J Phys: Condens Matter. 2004;16:S497–S530.
[18] Potapkin V, Chumakov AI, Smirnov GV, Celse J-P, Ruffer R, McCammon C, Dubrovinsky L. The ^{57}Fe synchrotron Mössbauer source at the ESRF. J Synchrotron Radiat. 2012;19:559–569.
[19] McCammon C, Kantor I, Narygina O, Rouquette J, Ponkratz U, Sergueev I, Mezouar M, Prakapenka V, Dubrovinsky L. Stable intermediate-spin ferrous iron in lower mantle perovskite. Nat Geosci. 2008;1:684–687.
[20] McCammon C, Dubrovinsky L, Narygina O, Kantor I, Wu X, Glazyrin K, Sergueev I, Chumakov A. Low-spin Fe^{2+} in silicate perovskite and a possible layer at the base of the lower mantle. Phys Earth Planet Inter. 2010;180:215–221.
[21] Narygina OV, Kantor IY, McCammon CA, Dubrovinsky LS. Electronic state of Fe^{2+} in (Mg,Fe)(Si,Al)O_3 perovskite and (Mg,Fe)SiO_3 majorite at pressures to 81 GPa and temperatures to 800K. Phys Chem Miner. 2010;37:407–415.
[22] Potapkin V, McCammon C, Glazyrin K, Kantor A, Kupenko I, Prescher C, Sinmyo R, Smirnov GV, Chumakov AI, Rüffer R, Dubrovinsky L. Effect of iron oxidation state on the electrical conductivity of the Earth's lower mantle. Nat Commun. 2012;4(1427):1–6.
[23] Rüffer R, Chumakov AI. Nuclear resonance beamline at ESRF. Hyperfine Interact. 1996;97/98:589–604.
[24] Prescher C, McCammon C, Dubrovinsky L. MossA – a program for analyzing energy-domain Mossbauer spectra from conventional and synchrotron sources. J Appl Crystallogr. 2012;45:329–331.
[25] Potapkin VB, Chumakov AI, Smirnov GV, Rüffer R, McCammon C, Dubrovinsky L. Angular, spectral and temporal properties of nuclear radiation from the ^{57}Fe Synchrotron Mössbauer source. Phys Rev A. 2012;A 86, 053808-1–5.

[26] Shvyd'ko YV. MOTIF: evaluation of time spectra for nuclear forward scattering. Hyperfine Interact. 2000;125: 173–188.

[27] McCammon CA, Rubie DC, Ross II CR, Seifert F, O'Neill HSC. Mössbauer spectra of $^{57}Fe_{0.05}Mg_{0.95}SiO_3$ perovskite at 80 and 298 K. Amer Mineral. 1992;77:894–897.

[28] McCammon CA. Mössbauer spectroscopy of quenched high-pressure phases: investigating the earth's interior. Hyper Inter. 1994;90:89–105.

[29] Fei Y, Virgo D, Mysen BO, Wang Y, Mao HK. Temperature dependent electron delocalization in $(Mg,Fe)SiO_3$ perovskite. Amer Mineral. 1994;79:826–837.

[30] Lauterbach S, McCammon CA, van Aken P, Langenhorst F, Seifert F. Mössbauer and ELNES spectroscopy of $(Mg,Fe)(Si,Al)O_3$ perovskite: a highly oxidised component of the lower mantle. Contrib Mineral Petrol. 2000;138: 17–26.

[31] Lin J-F, Watson H, Vankó G, Alp EE, Prakapenka VB, Dera P, Struzhkin VV, Kubo A, Zhao J, McCammon C, Evans WJ. Predominant intermediate-spin ferrous iron in lowermost mantle post-perovskite and perovskite. Nat Geosci. 2008;1:688–691.

[32] Jackson JM, Sturhahn W, Shen G, Zhao J, Hu M, Errandonea D, Bass JD, Fei Y. A synchrotron Mössbauer spectroscopy study of $(Mg,Fe)SiO_3$ perovskite up to 120 GPa. Amer Mineral. 2005;90:199–205.

[33] Grocholski B, Shim S-H, Sturhahn W, Zhao J, Xiao Y, Chow PC. Spin and valence states of iron in $(Mg_{0.8}Fe_{0.2})SiO_3$ perovskite. Geophys Res Lett. 2009;36:L24303-1–5.

[34] Lin J-F, Alp EE, Mao Z, Inoue T, McCammon C, Xiao Y, Chow P, Zhao J. Electronic spin states of ferric and ferrous iron in the lower-mantle silicate perovskite. Amer Mineral. 2012;97:592–597.

[35] Keppler H, McCammon CA, Rubie DC. Crystal field and charge transfer spectra of $(Mg,Fe)SiO_3$ perovskite. Amer Mineral. 1994;79:1215–1218.

[36] McCammon CA. The crystal chemistry of ferric iron in $Mg_{0.95}Fe_{0.05}SiO_3$ perovskite as determined by Mössbauer spectroscopy in the temperature range 80–293 K. Phys Chem Miner. 1998;25:292–300.

[37] Cohen RE, Mazin II, Isaak DG. Magnetic collapse in transition metal oxides at high pressure: implications for the Earth. Science. 1997;275:654–657.

[38] Li L, Brodholt JP, Stackhouse S, Weidner DJ, Alfredsson M, Price GD. Electronic spin state of ferric iron in Al-bearing perovskite in the lower mantle. Geophys Res Lett. 2005;32:L17307-1–4.

[39] Zhang F, Oganov AR. Valence state and spin transitions of iron in Earth's mantle silicates. Earth Planet Sci Lett. 2006;249:436–443.

[40] Stackhouse S, Brodholt JP, Price GD. Electronic spin transitions in iron-bearing $MgSiO_3$ perovskite. Earth Planet Sci Lett. 2007;253:282–290.

[41] Fang C, Ahuja R. Local structure and electronic-spin transition of Fe-bearing $MgSiO_3$ perovskite under conditions of the Earth's lower mantle. Phys Earth Planet Inter. 2008;166:77–82.

[42] Bengtson A, Persson K, Morgan D. Ab initio study of the composition dependence of the pressure induced spin crossover in perovskite $(Mg_{1-x},Fe_x)SiO_3$. Earth Planet Sci Lett. 2008;265:535–545.

[43] Umemoto K, Wentzcovitch RM, Yu YG, Requist R. Spin transition in $(Mg,Fe)SiO_3$ perovskite under pressure. Earth Planet Sci Lett. 2008;276:198–206.

[44] Bengtson A, Li J, Morgan D. Mössbauer modeling to interpret the spin state of iron in $(Mg,Fe)SiO_3$ perovskite. Geophys Res Lett. 2009;36:L15301-1–5.

[45] Hsu H, Umemoto K, Blaha P, Wentzcovitch RM. Spin states and hyperfine interactions of iron in $(Mg,Fe)SiO_3$ perovskite under pressure. Earth Planet Sci Lett. 2010;294:19–26.

[46] Hsu H, Umemoto K, Wu Z, Wentzcovitch RM. Spin-state crossover of iron in lower-mantle minerals: results of DFT plus U investigations. In: Wentzcovitch RM, Stixrude L, editors. Theoretical and computational methods in mineral physics: geophysical applications. Chantilly, VA: Mineralogical Society of America; 2010. p. 169–199.

[47] Umemoto K, Hsu H, Wentzcovitch RM. Effect of site degeneracies on the spin crossovers in $(Mg, Fe)SiO_3$ perovskite. Phys Earth Planet Inter. 2010;180:209–214.

[48] Hsu H, Blaha P, Cococcioni M, Wentzcovitch RM. Spin-state crossover and hyperfine interactions of ferric iron in $MgSiO_3$ perovskite. Phys Rev Lett. 2011;106:118501-1–4.

[49] Wentzcovitch RM, Hsu H, Umemoto K. First-principles studies of spin-state crossovers of iron in perovskite. Eur J Mineral. 2012;24:851–862.

[50] Stackhouse S. The spin deep within. Nat Geosci. 2008;1:648–650.

[51] Ingalls R. Electric-field gradient tensor in ferrous compounds. Phys Rev. 1964;133:A787–A795.

[52] Huggins FE. The 3d levels of ferrous iron in silicate garnets. Amer Mineral. 1975;60:316–319.

[53] Hirose K. Postperovskite phase transition and its geophysical implications. Rev Geophys. 2006;44:RG3001.

[54] Hernlund JW, Thomas C, Tackley PJ. A doubling of the post-perovskite phase boundary and structure of the Earth's lowermost mantle. Nature. 2005;434:882–886.

[55] Glazyrin, K. Iron in oxides, silicates and alloys under extreme pressure-temperature conditions [PhD thesis]. University of Bayreuth; 2011. Available from: http://opus.ub.uni-bayreuth.de/opus4-ubbayreuth/files/732/Dissertation_Glazyrin.pdf